Electronic Supplementary Material (ESI) for Catalysis Science & Technology.

EDTA derived Graphene supported Porous Cobalt Hexacyanoferrate nanospheres as a highly electroactive nanocomposite for Hydrogen Peroxide sensing

Ramu Banavath [a, b,*], *Rohit Srivastava* [b], *Parag Bhargava* [a*]

a-Department of Metallurgical and Materials Science, Indian Institute of Technology-Bombay, Mumbai, India, 400076
b-Department of Biosciences and Bioengineering, Indian Institute of Technology-Bombay, Mumbai, India, 400076

*Corresponding author.
E-mail address: ramubanavath@iitb.ac.in (Ramu Banavath), pbhargava@iitb.ac.in (Parag Bhargava)
Mailing address: IIT Bombay, Powai, Maharashtra, India, 400076

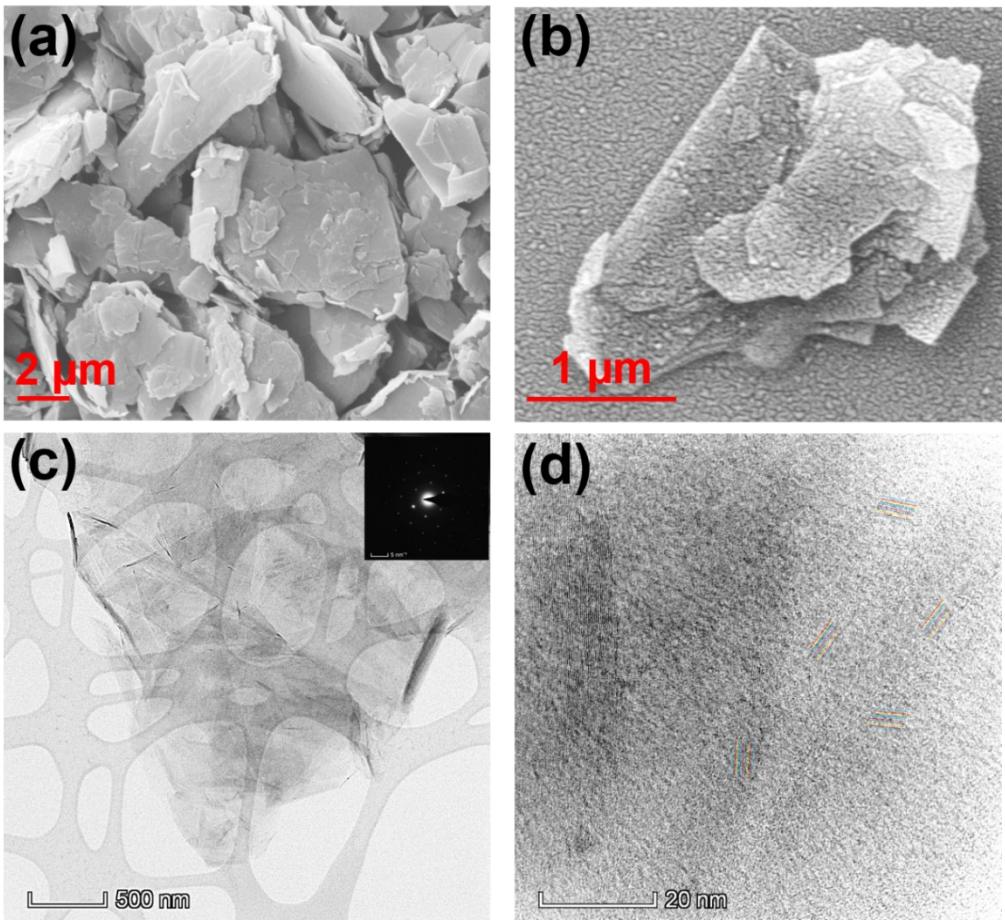

Figure S 1: - (a) FEG-SEM image of Natural Graphite, (b) FEG-SEM image of exfoliated graphene, (c, d) FEG-TEM images of exfoliated graphene.

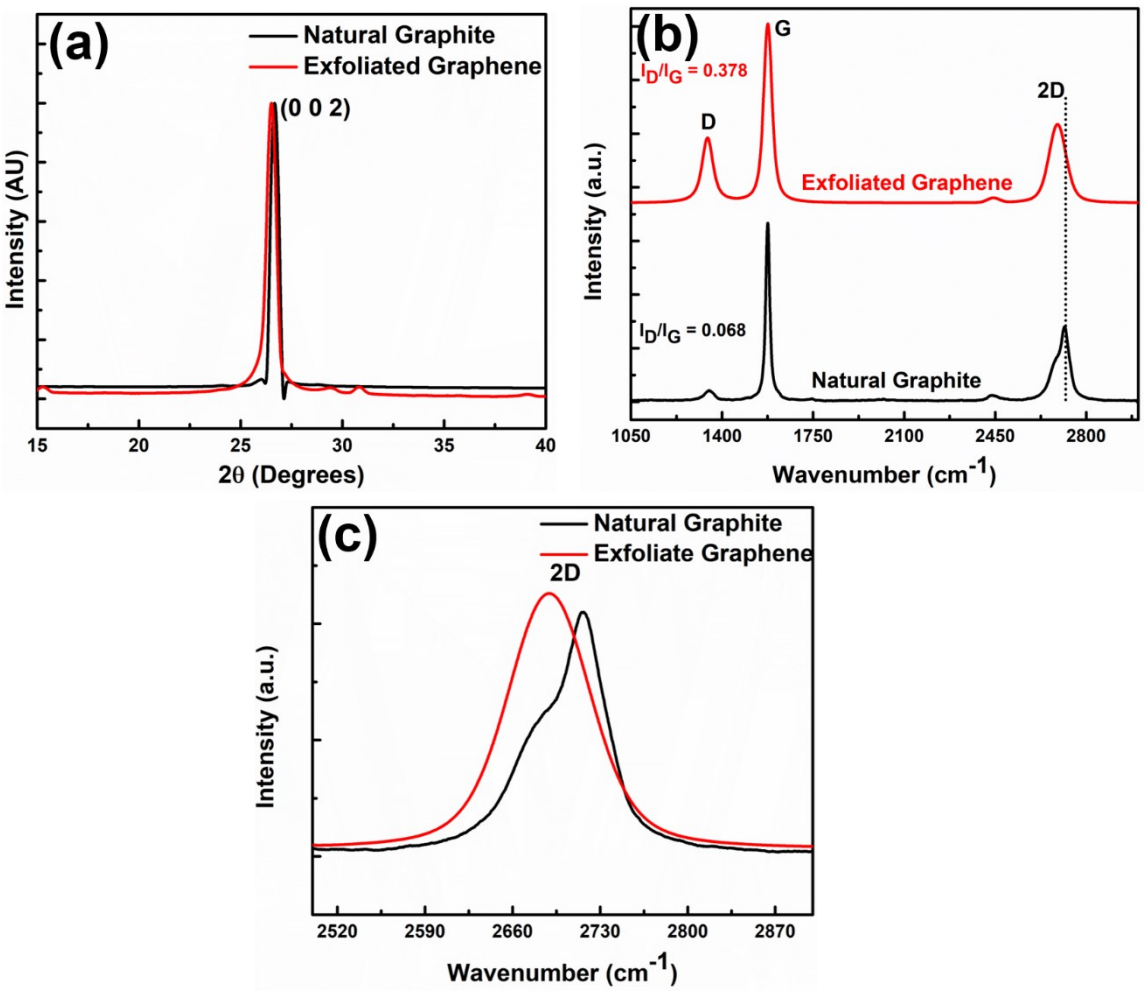

Figure S 2: - (a) X-ray diffractometry spectra comparison of exfoliated graphene with natural graphite, (b, c) Raman spectroscopy of exfoliated graphene and its comparison with natural graphite.

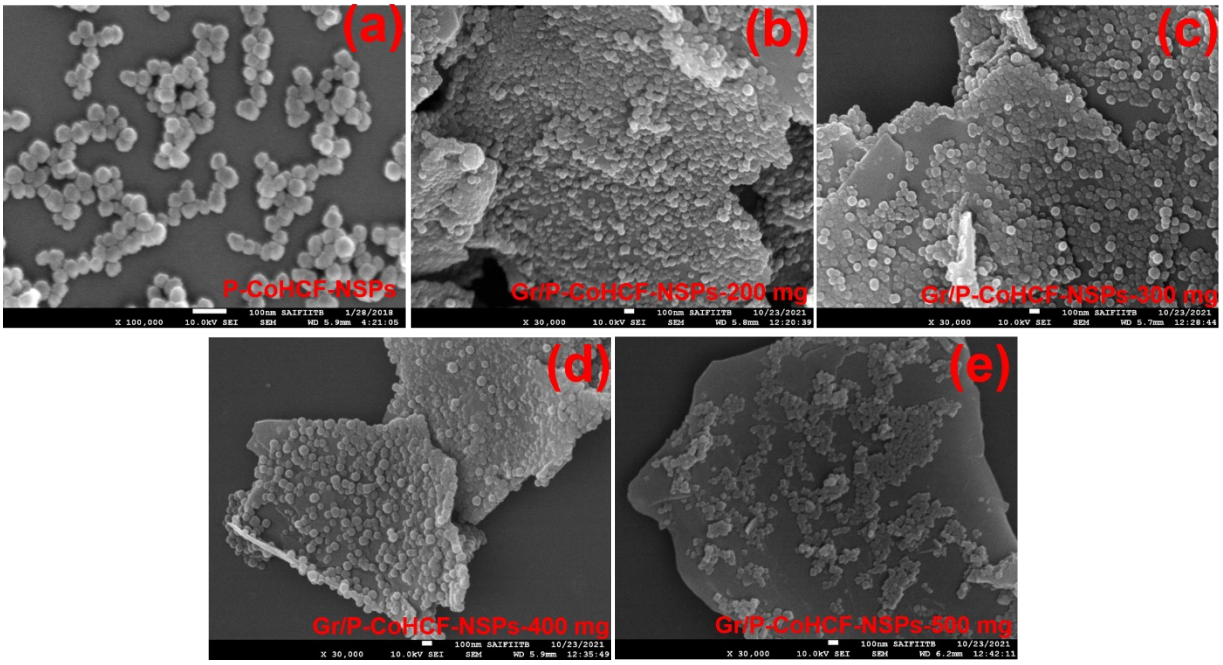

Figure S 3: - FEG-SEM images of P-CoHCF-NSPs and Gr/P-CoHCF-NSPs composites prepared at different concentrations of exfoliated graphene.

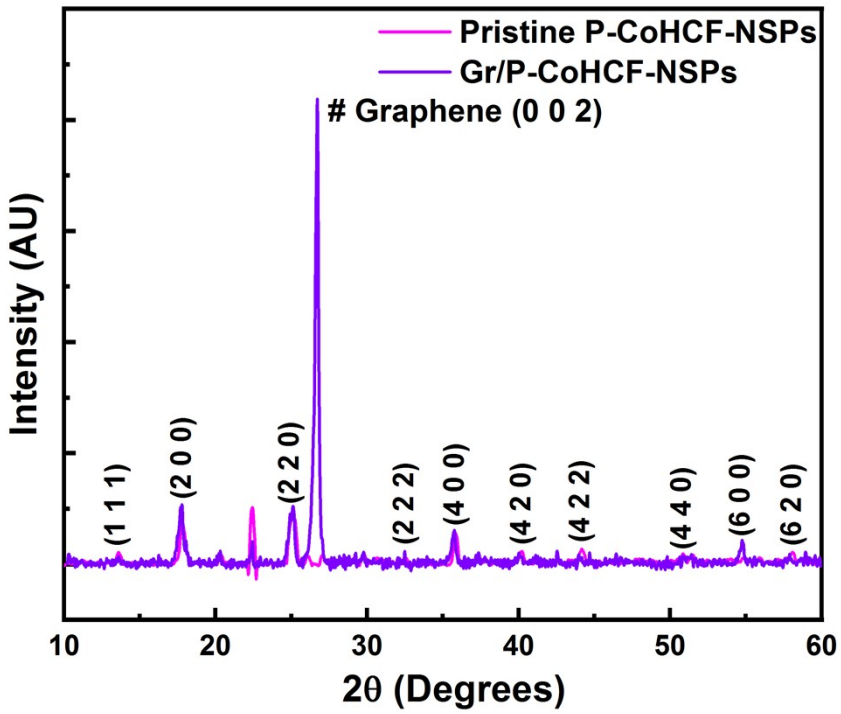

Figure S 4: - XRD peaks intensity comparison for Pristine P-CoHCF-NSPs and Gr/P-CoHCF-NSPs composite.

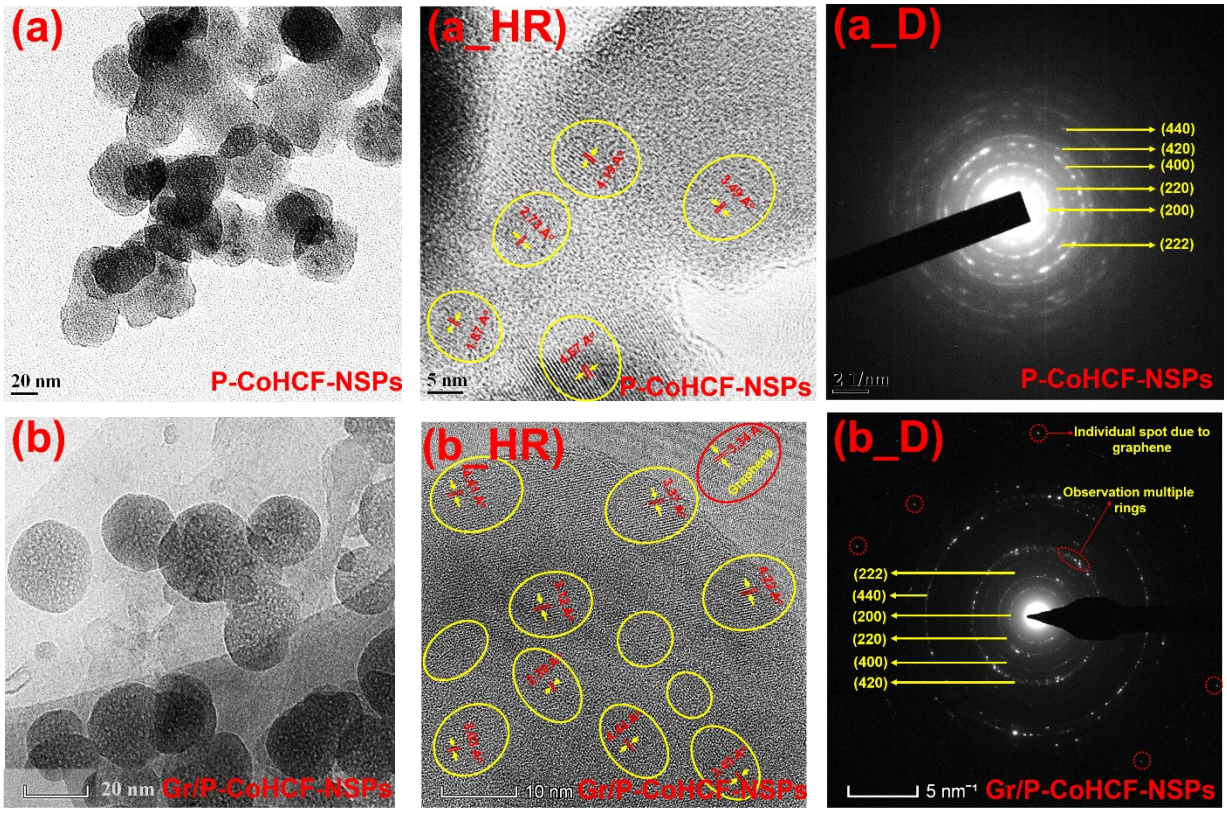

Figure S 5: - (a, a_HR, a_D) TEM images of of P-CoHCF-NSPs, and (b, b_HR, b_D) TEM images of Gr/P-CoHCF-NSPs composite.

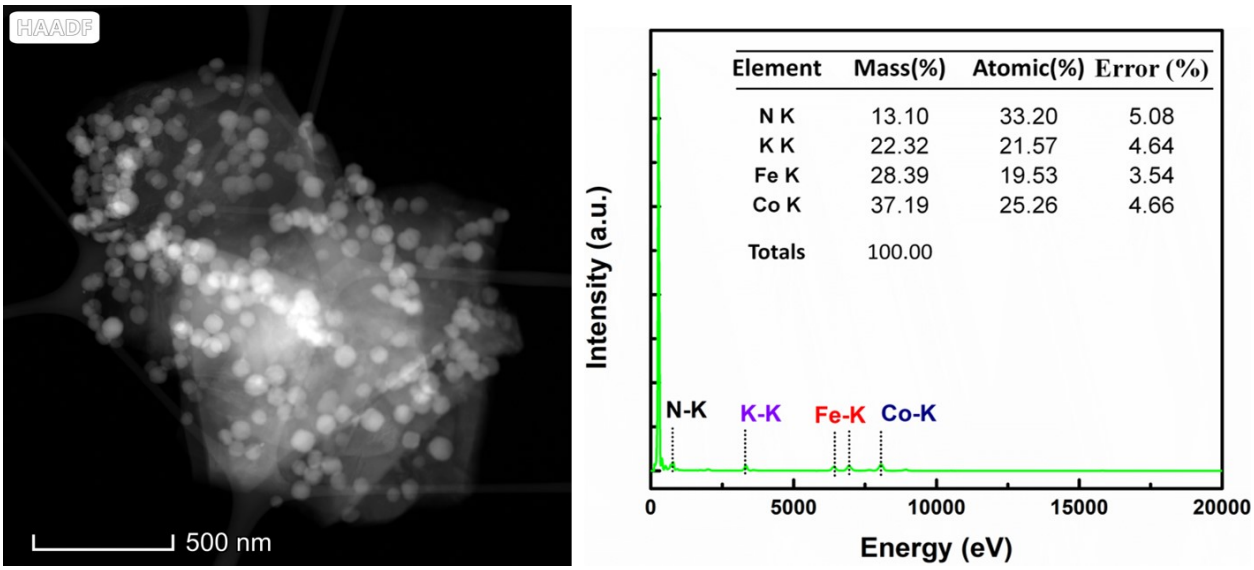

Figure S 6: - EDS spectra of Gr/P-CoHCF-NSPs found from HAADF-STEM elemental mapping.

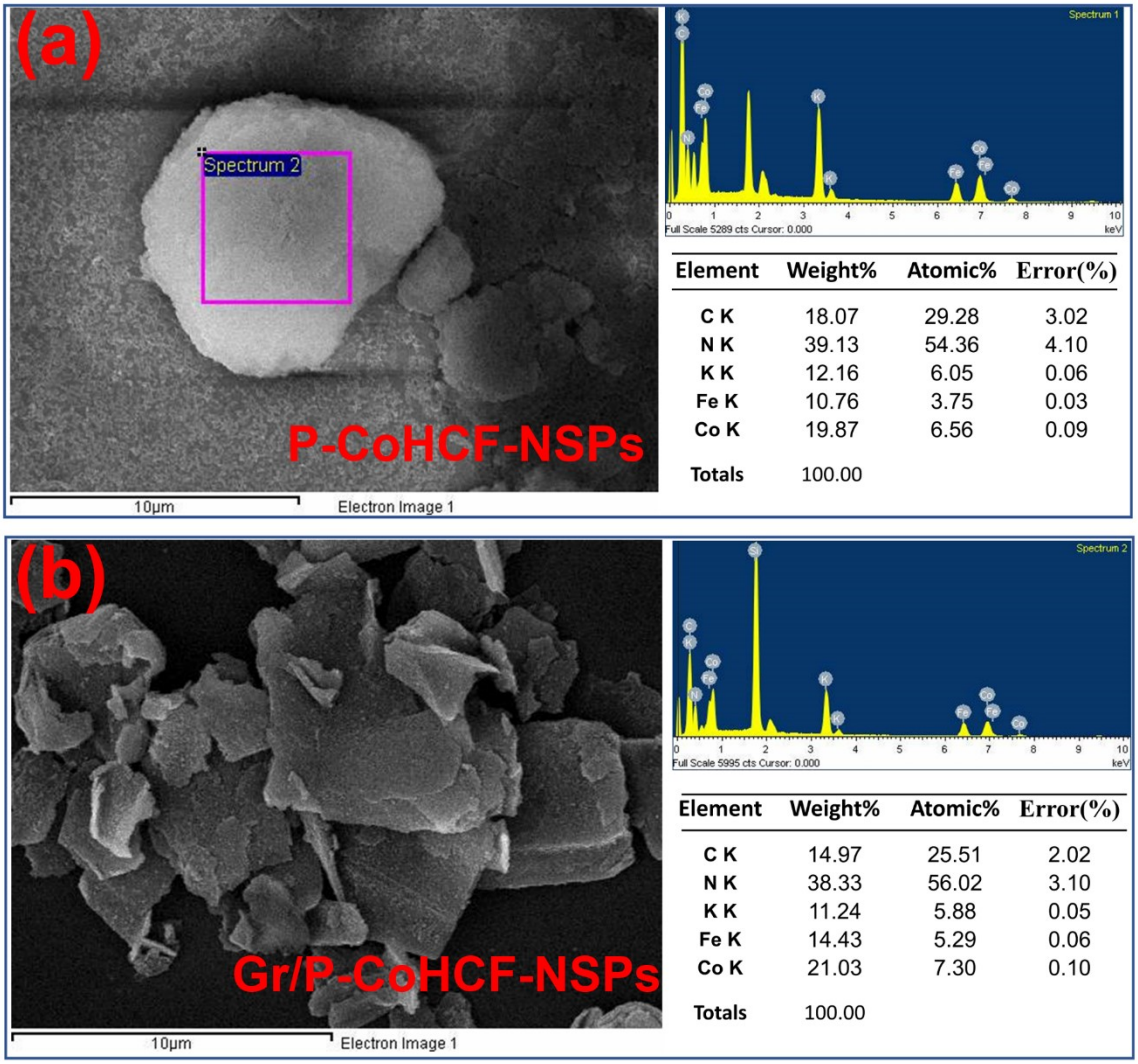

Figure S 7: - EDS of pristine P-CoHCF-NSPs and Gr/P-CoHCF-NSPs composite prepared with 400 mg graphene.

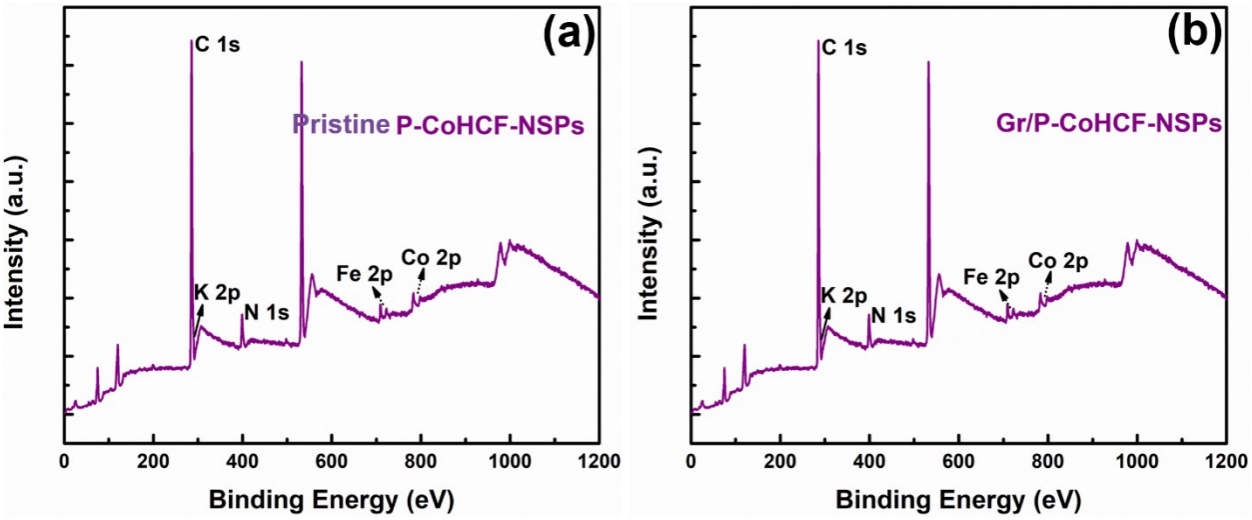

Figure S 8: - XPS wide spectrums for pristine P-CoHCF-NSPs (a), and Gr/P-CoHCF-NSPs based composite.

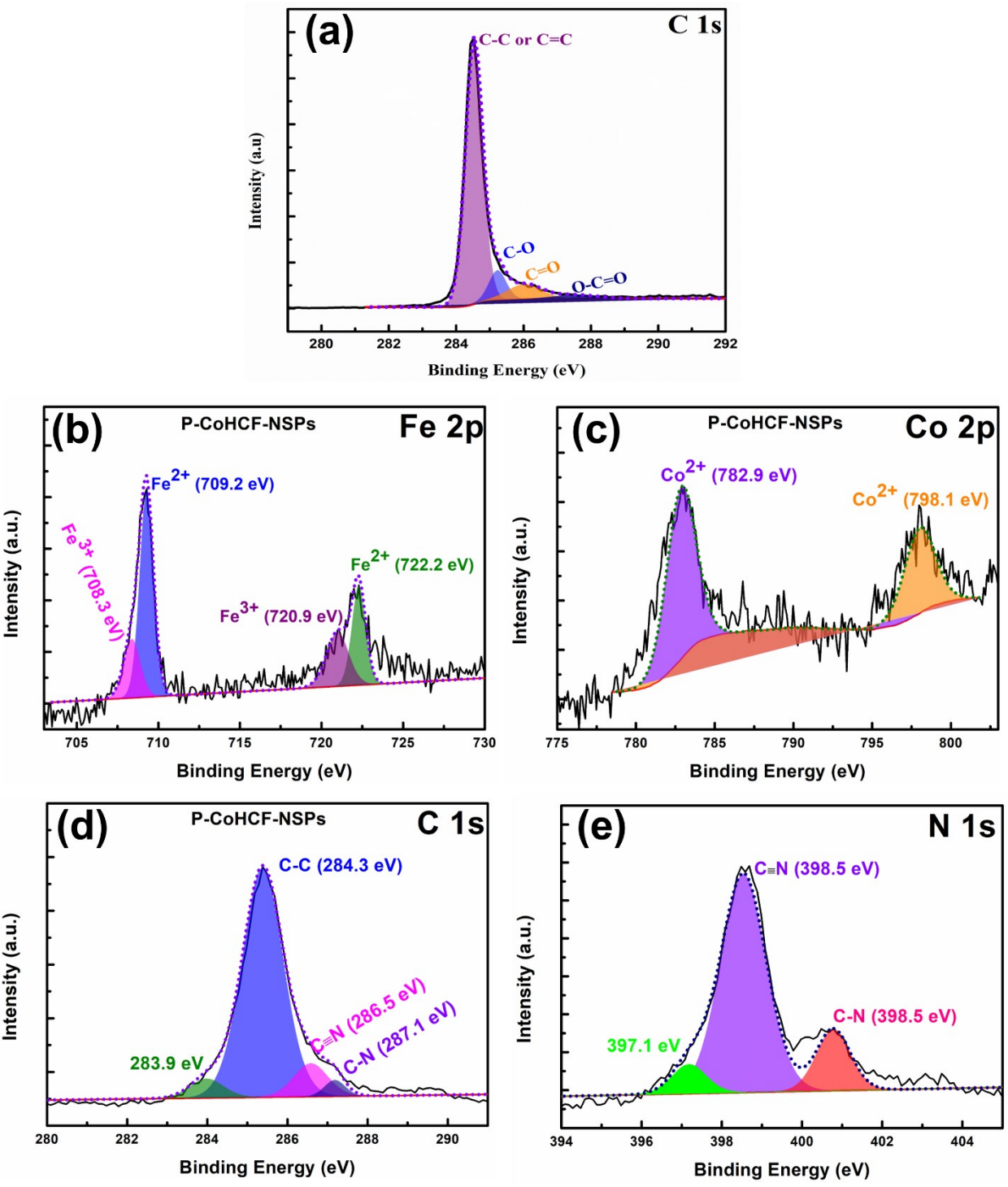

Figure S 9: - (a) XPS spectra of exfoliated graphene, (b, c, d, e) High-resolution XPS spectra of Fe, Co, C, and N of pristine P-CoHCF-NSPs.

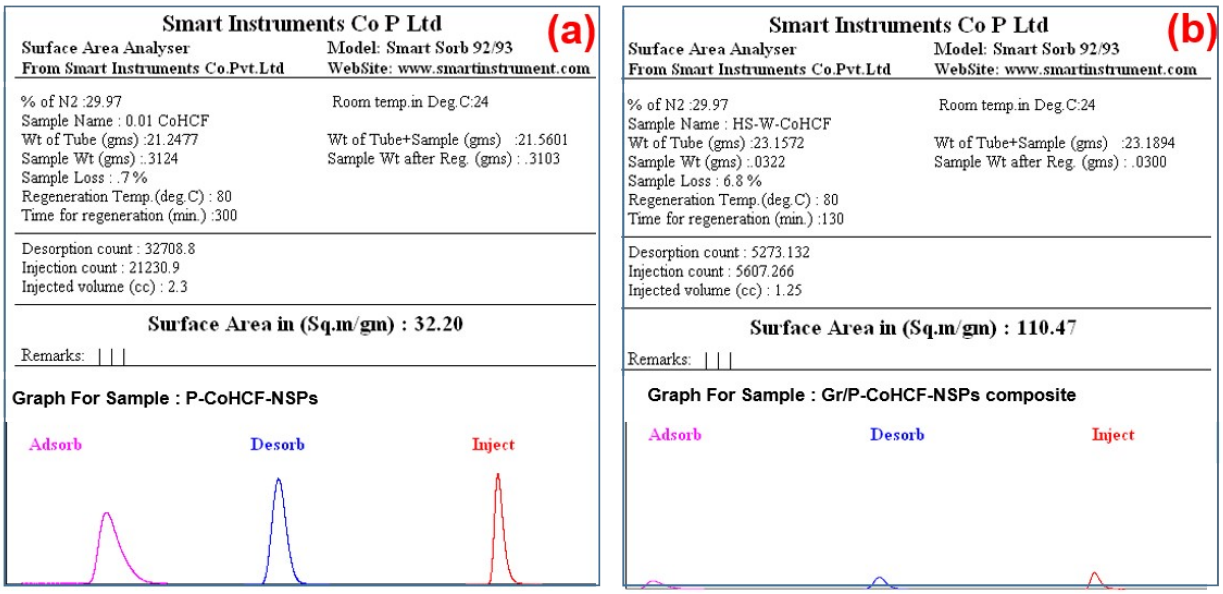

Figure S 10: - Specific surface area of P-CoHCF-NSPs and Gr/P-CoHCF-NSPs composite calculated by single point BET .

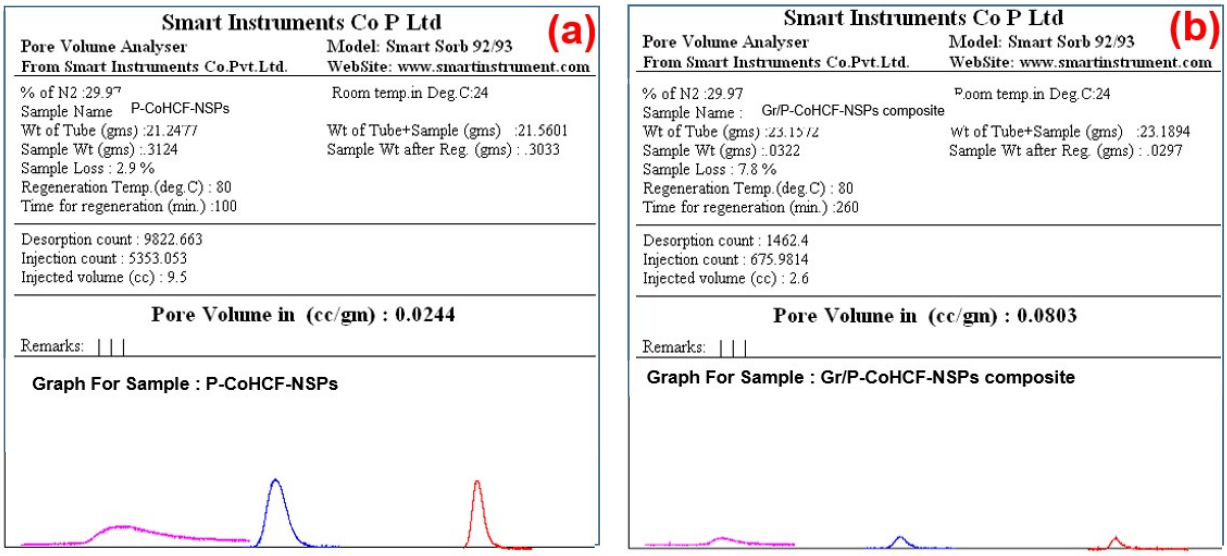

Figure S 11: - Pore volume of P-CoHCF-NSPs and Gr/P-CoHCF-NSPs composite calculated by single point BET .

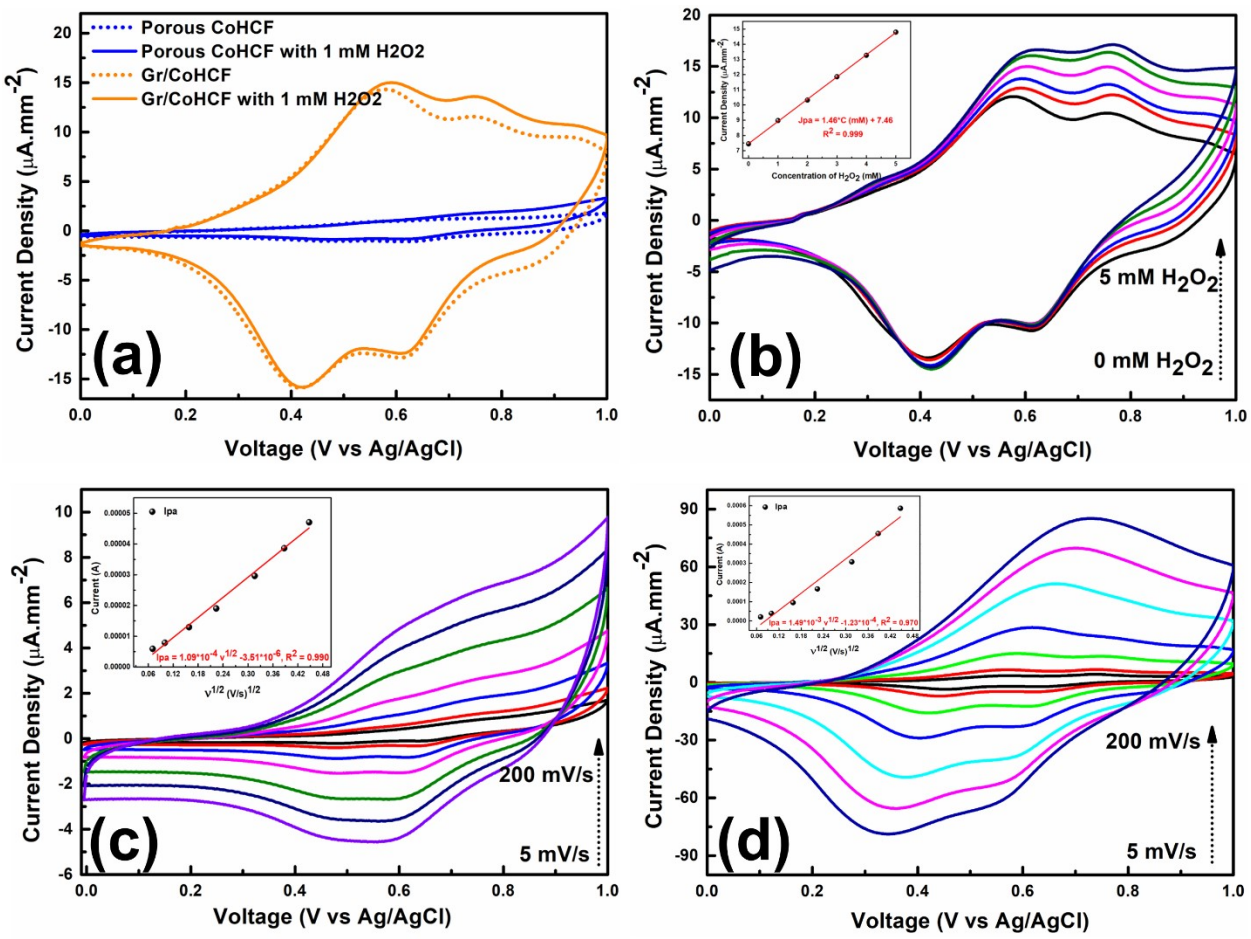

Figure S 12: - All CV characterizations of 27 µl composite ink modified glassy carbon electrodes (a) CV comparison with pristine P-CoHCF-NSPs in 1 mM H_2O_2, (b) CV for different concentrations of H_2O_2, (c, d) CV can rate comparison of composite with P-CoHCF-NSPs in 1 mM H_2O_2 containing PBS.

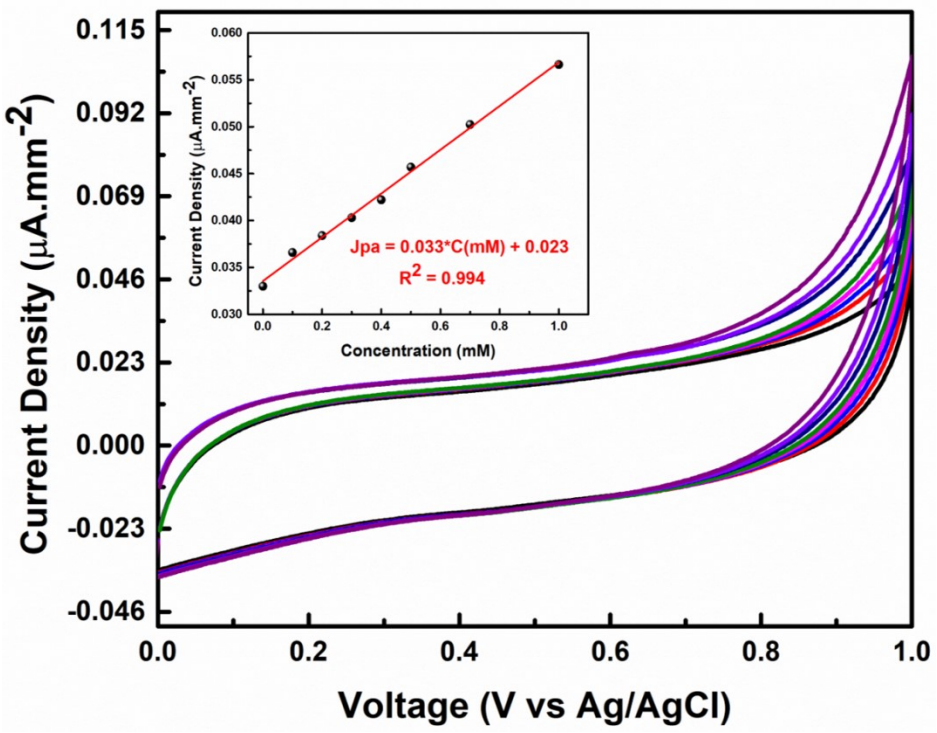

Figure S 13: - CV of blank GCE in the presence of different concentrations of H2O2 at the SR of 25 mV/s.

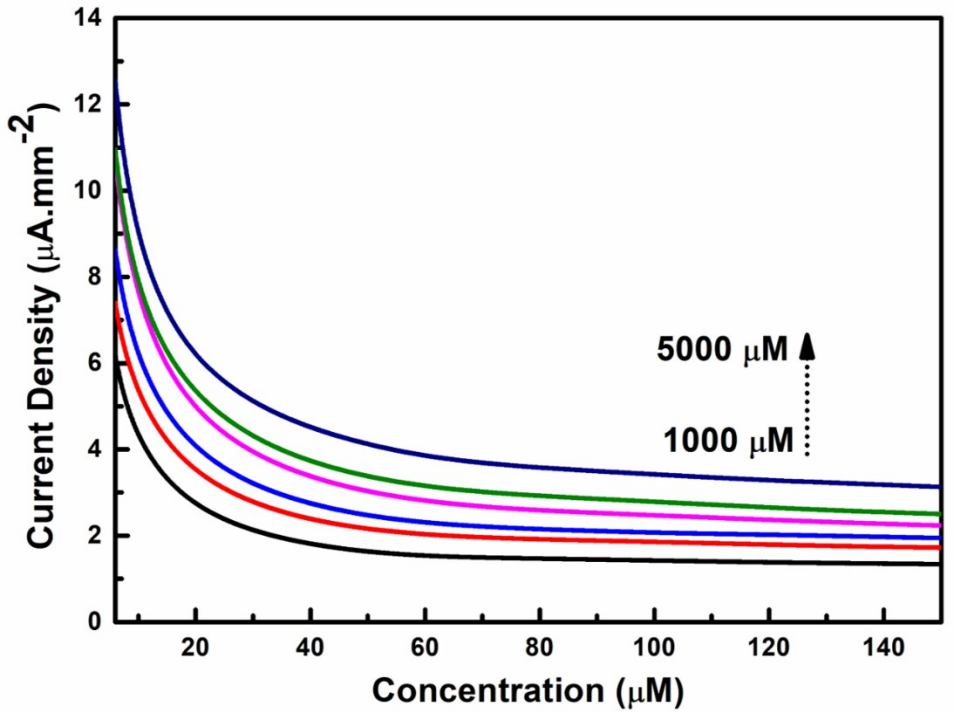

Figure S 14: - Chronoamperometry of Gr/P-CoHCF-NSPs composite based H_2O_2 sensor for high concentrations of H_2O_2.

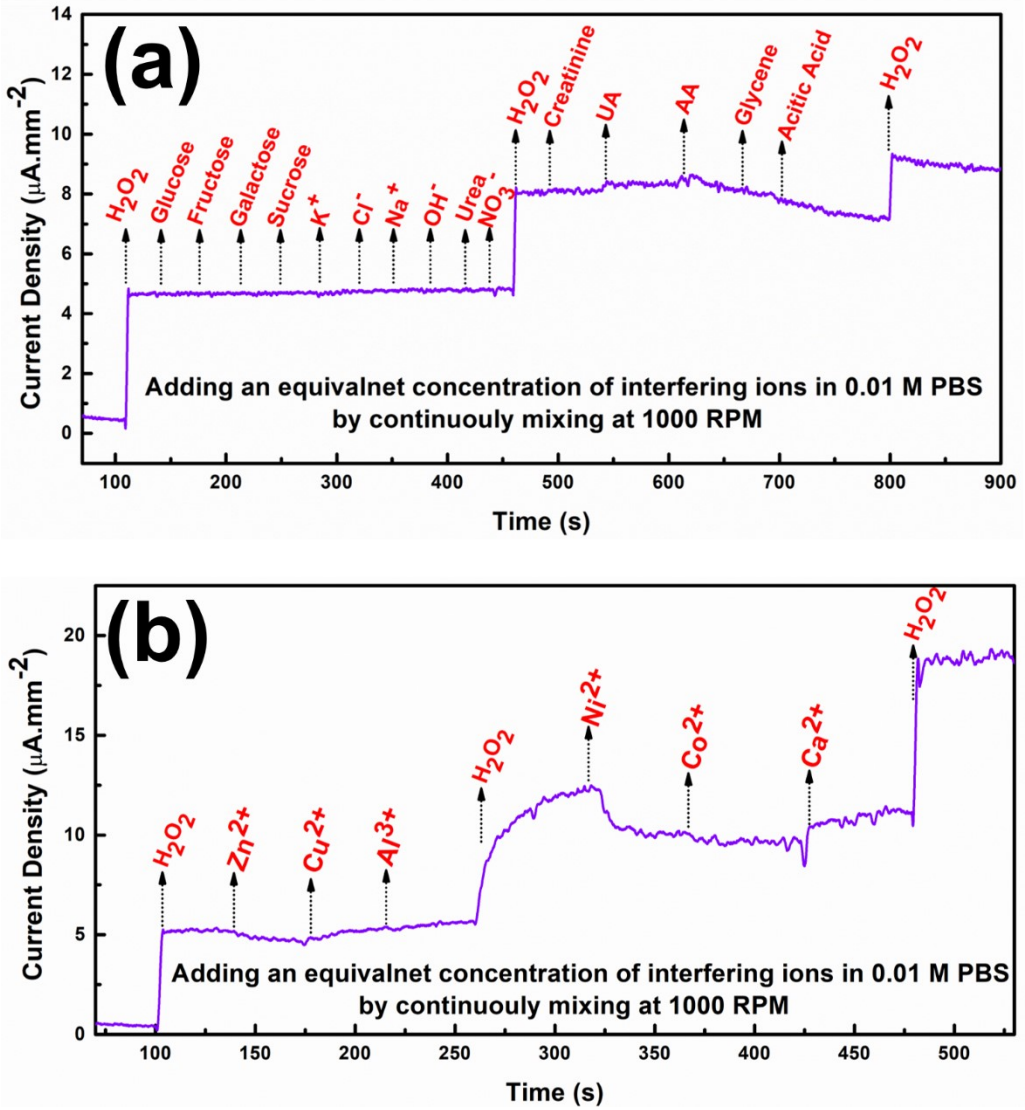

Figure S 15: - Amperometric plots for Interference study of Gr/P-CoHCF-NSPs composite based H_2O_2, (a) For common interfering ions, (b) For metal based interfering ions.

Table S1: -Gr/P-CoHCF-NSPs based H_2O_2 Sensor parameters with recently published work.

Electrode	Sensitivity ($\mu A.mM^{-1}\ cm^{-2}$)	LOD (μM)	Linear Range (mM)	Ref
ZnO_3-CuO_7	1.11	2.4	0.003 – 0.53	[1]
MWCNTs/MnO_2	13.9	6.97	0.1 – 20.7	[2]
AgNp@GNR	-	20	0.05 – 5	[3]
Black Berry Ag Nano	51.28	1.06	0.001 – 0.29	[4]
AuNPs/PB/GO	87.6	1.3	0.03 – 5.4	[5]
NiO/Carbon Foam	23.3	0.01	0.2 – 3.75	[6]
MoS2/Au-Pd	184	0.16	0.0008 - 10	[7]
Hollow CuO_x/NiO_y	271	0.9	0.0003 - 9	[8]
Au/Cu Nanostructures	133.74	10.93	0.05 - 10	[9]
PDA-CNT/Fe_3O_4 Cs	316.27	6	0.006 – 2.057	[10]
C/V_2O_5 Nanosheets	204.64	1.7	0.005 – 1.5	[11]
Meso-C/ZnO/GCE	464	6.25	50 - 981	[12]
Hollow Ni/NiO@C microspheres	32.09	0.9	- 80.7	[13]
Gr/P-CoHCF-NSPs/GCE	914	1.0	0.001 – 5.0	This work

Table S2: - Recovery study of fabricated Gr/P-CoHCF-NSPs composite based H_2O_2 sensor.

Concentration of H_2O_2 (µM)	Output Current Density in PBS (µA.mm^{-2})	Output Current Density in Lake water (µA.mm^{-2})	Percentage of recovery (%)	% RCD
20	0.5111	0.5237	102.4	3.1
50	0.6763	0.6861	101.4	1.5
100	1.0999	1.0727	97.5	2.8
1000	6.6300	6.3775	96.2	3.9

References: -

[1] S. Daemi, S. Ghasemi, A. Akbar Ashkarran, Electrospun CuO-ZnO nanohybrid: Tuning the nanostructure for improved amperometric detection of hydrogen peroxide as a non-enzymatic sensor, J. Colloid Interface Sci. 550 (2019) 180–189. https://doi.org/10.1016/j.jcis.2019.04.091.

[2] M. Dinesh, C. Revathi, Y. Haldorai, R.T. Rajendra Kumar, Birnessite MnO2 decorated MWCNTs composite as a nonenzymatic hydrogen peroxide sensor, Chem. Phys. Lett. 731 (2019) 136612. https://doi.org/10.1016/j.cplett.2019.136612.

[3] V. Stanković, S. Đurđić, M. Ognjanović, J. Mutić, K. Kalcher, D.M. Stanković, A novel nonenzymatic hydrogen peroxide amperometric sensor based on AgNp@GNR nanocomposites modified screen-printed carbon electrode, J. Electroanal. Chem. 876 (2020) 2–7. https://doi.org/10.1016/j.jelechem.2020.114487.

[4] M.L.N. Thi, V.T. Pham, Q.B. Bui, P.H. Ai-Le, H.T. Nhac-Vu, Novel nanohybrid of blackberry-like gold structures deposited graphene as a free-standing sensor for effective hydrogen peroxide detection, J. Solid State Chem. 286 (2020). https://doi.org/10.1016/j.jssc.2020.121299.

[5] X. Liu, X. Zhang, J. Zheng, One-pot fabrication of AuNPs-Prussian blue-Graphene oxide hybrid nanomaterials for non-enzymatic hydrogen peroxide electrochemical detection, Microchem. J. 160 (2021) 105595. https://doi.org/10.1016/j.microc.2020.105595.

[6] M. Liu, M. An, J. Xu, T. Liu, L. Wang, Y. Liu, J. Zhang, Three-dimensional carbon foam supported NiO nanosheets as non-enzymatic electrochemical H2O2 sensors, Appl. Surf. Sci. 542 (2021) 148699. https://doi.org/10.1016/j.apsusc.2020.148699.

[7] X. Li, X. Du, Molybdenum disulfide nanosheets supported Au-Pd bimetallic nanoparticles for non-enzymatic electrochemical sensing of hydrogen peroxide and glucose, Sensors Actuators, B Chem. 239 (2017) 536–543. https://doi.org/10.1016/j.snb.2016.08.048.

[8] L. Long, X. Liu, L. Chen, D. Li, J. Jia, A hollow CuOx/NiOy nanocomposite for amperometric and non-enzymatic sensing of glucose and hydrogen peroxide, Microchim. Acta. 186 (2019) 5–10. https://doi.org/10.1007/s00604-018-3183-x.

[9] A. Ngamaroonchote, Y. Sanguansap, T. Wutikhun, K. Karn-orachai, Highly branched gold–copper nanostructures for non-enzymatic specific detection of glucose and hydrogen peroxide, Microchim. Acta. 187 (2020) 1–12. https://doi.org/10.1007/s00604-020-04542-x.

[10] Y. Zhao, D. Huo, L. Jiang, S. Zhou, M. Yang, C. Hou, Synthesis of dopamine-derived N-doped carbon nanotubes/Fe3O4 composites as enhanced electrochemical sensing platforms for hydrogen peroxide detection, Microchim. Acta. 187 (2020). https://doi.org/10.1007/s00604-020-04575-2.

[11] S. Chen, C. Wang, X. Lu, Fabrication of two-dimensional carbon/V2O3 composite nanosheets and their application for electrochemical sensing, Compos. Commun. 27 (2021) 100842. https://doi.org/10.1016/j.coco.2021.100842.

[12] M.A. Rashed, M. Faisal, F.A. Harraz, M. Jalalah, M. Alsaiari, S.A. Alsareii, A Highly Efficient Nonenzymatic

Hydrogen Peroxide Electrochemical Sensor Using Mesoporous Carbon Doped ZnO Nanocomposite, J. Electrochem. Soc. 168 (2021) 027512. https://doi.org/10.1149/1945-7111/abe44b.

[13] X. Ma, K. lai Tang, M. Yang, W. Shi, W. Zhao, Metal–organic framework-derived yolk–shell hollow Ni/NiO@C microspheres for bifunctional non-enzymatic glucose and hydrogen peroxide biosensors, J. Mater. Sci. 56 (2021) 442–456. https://doi.org/10.1007/s10853-020-05236-8.